Deterministic Multi-Zone Ice Accretion Modeling

K. Yamaguchi* and R.J. Hansman, Jr.**
Department of Aeronautics and Astronautics
Massachusetts Institute of Technology
Cambridge, MA

M. Kazmierczak†
Department of Mechanical, Industrial, and Nuclear Engineering
University of Cincinnati
Cincinnati, OH

Abstract

A deterministic surface roughness transition model was proposed and implemented in the Multi-Zone version of the LEWICE ice accretion prediction code for glaze ice conditions. The transition model links the smooth/rough surface roughness transition with the laminar to turbulent boundary layer transition. The initial transition location is determined by boundary layer stability in the smooth laminar region. The subsequent upstream migration of the transition region is caused by a surface water bead formation process and controlled by the surface water flux out of the laminar/smooth region. The effectiveness of the surface roughness transition model was tested by comparing predictions of the deterministic Multi-Zone LEWICE code with experimental ice accretions for cylinder and airfoil geometries. Good agreement was achieved between the deterministic Multi-Zone LEWICE predictions and the experimental ice shapes. Some numerical difficulties were encountered due to limitations of the flow field code used in LEWICE. The glaze ice shapes were found to be sensitive to the laminar surface roughness and bead thickness parameters which controlled the transition location. The ice shapes were found to be insensitive to the turbulent surface roughness.

* Research Assistant, Student Member AIAA
** Associate Professor, Associate Fellow AIAA
† Assistant Professor, Member AIAA

1. Introduction

1.1. Background

Glaze icing presents the most difficult challenge for aircraft ice accretion modeling. In glaze icing, which normally occurs at temperatures near freezing or at high liquid water contents, there is insufficient convective heat transfer to remove all of the latent heat of freezing of the impinging supercooled water droplets. Consequently, the local ice accretion rate is controlled by the local convective heat transfer.

The local convective heat transfer from a surface is known to be strongly dependent on the ice surface roughness and the boundary layer behavior.[1,2] Because of the importance of heat transfer on the ice accretion rate, the surface roughness and it's influence on boundary layer transition becomes an important factor in modelling glaze ice accretion. Current analytical models such as LEWICE generally assume that the surface roughness is uniform, and the effective sand grain roughness, k_s, is used as an input parameter in the code.[3] The magnitude of the roughness parameter is normally determined empirically by comparison to experimental ice accretions. The erratic performance of glaze ice accretion models and the empirical manner in which the surface roughness is treated indicate the need for a more deterministic treatment of the surface roughness.

1.2. Experimental Observations

In prior experiments, detailed observations of accreting ice surface roughness were made at several icing facilities.[4] In one series of experiments conducted at the B.F. Goodrich Ice Protection Research Tunnel, a set of well defined ice shapes were recorded using high magnification microvideo cameras and a laser light sheet to accurately identify the plane of focus and the surface roughness.

These detailed photographic analyses of the accreting ice surfaces, along with the pioneering work by Olsen,[5] have revealed regions with distinct surface

roughness characteristics. The different surface roughness regions include a smooth region centered about the stagnation line, where surface water flow was observed for some cases, and a rough region downstream of the smooth region. The location of smooth to rough zones as a function of time have been studied in detail using a laser light sheet, which enabled an accurate observation of surface roughness and the behavior of the smooth to rough transition point.[2] In general, the rough to smooth transition point is observed to propagate towards the stagnation region with time. These observations are consistent with a model which couples the formation of water beads on the ice surface with the rough/smooth transition and the laminar/turbulent boundary layer transition.

1.3. Multi-Zone Model

Based on the experimental observations of ice formation in glaze ice regime, a Multi-Zone model, in which the accreting ice surface is divided into two or more discrete zones with varying surface roughness and water behavior, was proposed.[6]

In the simplest version of the Multi-Zone model, the surface is divided into two zones, the smooth zone and the rough zone. In the smooth zone, corresponding to the region observed to be centered about the stagnation point, the surface is smooth and uniformly wet with thin water film. Here, the convective heat transfer is insufficient to remove all of the latent heat of freezing, and surface water runback has been observed, indicating that the simple water runback model used in the original LEWICE implementation may be valid.[7]

In the rough zone, corresponding to the region found downstream of the smooth zone, the surface was observed to be considerably rougher. Here, the heat transfer is enhanced due to the increased roughness and the turbulent boundary layer. Experimental observations have indicated that in many cases there is no water runback in the rough zone.

1.4. Initial Implementation of the Multi-Zone Model in LEWICE Ice Accretion Prediction Code

In order to evaluate the effectiveness of the Multi-Zone model, a simple two zone version of the model was implemented in the LEWICE code, based on the hypothesis that the smooth/rough transition location coincided with the laminar/turbulent boundary layer transition location. Because no deterministic model for the propagation of the transition point was available, the transition location between the smooth and rough regions was input to the code from the experimental data in the preliminary implementation.

Comparisons between the preliminary Multi-Zone model with the original LEWICE code and experimental ice shapes indicated that significant improvements in glaze ice accretion prediction could be obtained with the Multi-Zone model using rough to smooth transition data from experimental observations.[6] These results indicated the need for a deterministic model of the rough to smooth transition behavior which could be incorporated in the Multi-Zone LEWICE code.

2. Deterministic Surface Roughness Transition Model

In order to implement the deterministic surface roughness model it was necessary to develop criteria for the initial location and subsequent propagation of the boundary between the smooth and rough zones. This smooth/rough transition has been investigated experimentally in several icing test facilities.[6,8] Based on the experimental studies a model of the surface roughness transition behavior of glaze ice has been proposed.

2.1. Initial Smooth/Rough Transition Location

Experimental observations indicated that the Reynolds number dependence of the *initial* location of surface roughness transition location correlated with the Reynolds number dependence of the boundary layer transition location. Therefore, it was hypothesized that the initial surface roughness transition is caused by the boundary layer transition. In this case, the initial smooth/rough transition will occur at the laminar/turbulent boundary layer transition point. Physically, it is thought that the low heat transfer in the laminar region causes a low freezing fraction which results in a relatively smooth surface water film. In the turbulent region, however, the increased heat transfer causes rapid freezing resulting in higher surface roughness.

It should be noted that the boundary layer transition location depends on the stability both of the laminar boundary layer which is influenced by the Reynolds number and of the stagnation region surface roughness. Increasing either tends to move the transition point toward the stagnation point. While the stagnation region is generally observed to be smooth, waves in the water film or small scale roughness can influence the initial location of the laminar/turbulent and hence the smooth/rough transition location.

2.2. Bead Formation and Propagation of the Transition Location

As discussed above, the smooth/rough transition point is typically observed to propagate toward the stagnation region with time. It has also been observed that higher surface water flow causes the rate of movement of the transition to increase.[8] Based on the

smooth/rough transition behavior and detailed observations of the surface water, it is hypothesized that the enhanced heat transfer in the turbulent region causes sufficient freezing to partially dry the surface and causes bead formation of unfrozen water which flows downstream from the laminar region. The bead formed at the interface of smooth and rough regions results in the increased roughness observed in the rough zone.

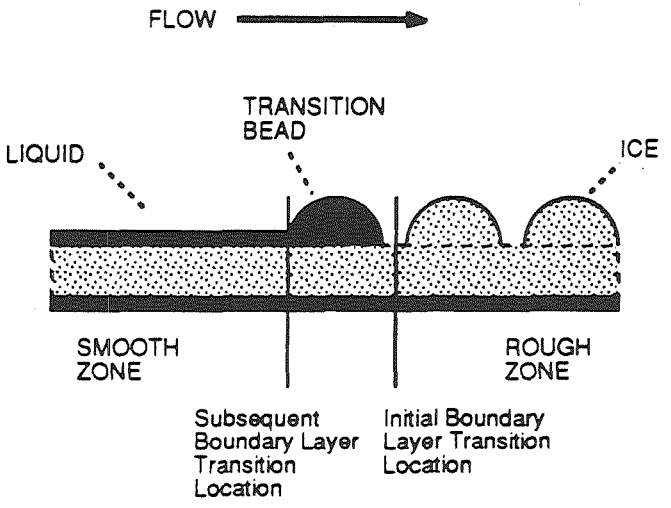

Fig. 1. Bead formation and boundary layer transition location

The mechanism for the propagation of the transition location is depicted in Fig. 1. The initial smooth/rough transition occurs because of the boundary layer transition as discussed above. As water flows from the upstream laminar region, a water bead is formed at the interface. The increased roughness of the bead causes the boundary layer to "trip" and transition to turbulent at the upstream edge of the bead. The, now turbulent, boundary layer enhances the heat transfer in the region where the bead has formed. With the increased heat transfer, the bead freezes forming rough ice. As the surface dries, beads begin to form further upstream. This process will repeat and the transition point will propagate toward the stagnation region as observed experimentally. By increasing the surface water flux, the rate of formation and growth of the interfacial beads are increased. This causes the observed increase in upstream propagation of the coupled rough/smooth-laminar/turbulent transition point with increasing surface water flux.

In some cases, splashing of impinging water drops has been observed to occur in the stagnation region. The splashing is thought to be limited to the thin water film in the smooth region. If significant splashing occurs, it will reduce the surface water flux into the transition region thereby slowing the propagation of transition.

2.3. Implementation in LEWICE Ice Accretion Prediction Code

Based on the above hypothesis that smooth/rough transition location coincides with the laminar/turbulent boundary layer transition location, a more physically realistic Multi-Zone model was implemented in the LEWICE code. Initially, a simple two-zone version of the Multi-Zone model was implemented through boundary layer transition, where the smooth and rough zones are considered to coincide with the regions of laminar and turbulent boundary layers.

For the initial time step, equivalent roughness element heights for both the laminar and turbulent zones are required as inputs. The laminar roughness height k_l, corresponding to the waviness of the laminar region water layer, is used to calculate a critical Reynolds number based on surface roughness size. This critical Reynolds determines the initial location of boundary layer transition.[2,9] Increasing the laminar region roughness will move the transition point forward. The turbulent roughness k_t is used to calculate the convective heat transfer coefficient which increases with roughness. By using two roughness element sizes, one for laminar region and one for the turbulent region, it is possible to control the transition location and turbulent heat transfer independently. The laminar roughness k_l is then used to determine the laminar to turbulent boundary layer transition location. The turbulent roughness k_t is used to calculate the heat transfer coefficient in the turbulent region.

This method more closely emulates the physical situation where two different roughnesses have been observed in the smooth and rough zones. In the laminar region, the roughness height corresponds to the roughness of the uniform water film. In the turbulent region, it corresponds to the roughness size observed in the rough region.

In the subsequent time steps, the location of smooth/rough transition was calculated based on the physical model depicted in Section 2.2. By assuming all the surface water mass flux is deposited into a bead at the boundary layer transition location, a relationship can be developed between surface water mass flux and the size of the bead formed. From mass conservation,

$$x = \frac{\dot{m}\,\Delta t}{\rho_\omega b}$$

where x is the distance covered by the bead along the surface, b is the bead thickness, $\dot{m}$ is the mass flux calculated by LEWICE, Δt is the time step used to run LEWICE, and ρ_ω is the density of water. With this

method, the bead thickness b, or the size of the bead, must be input. Based on the experimental observations of the surface roughness transition location, the thickness of the water film was estimated to be about 2 mm for the cases considered. An example of the transition propagation calculated using this method is compared with experimentally observed data in Fig. 2 for a 1" diameter cylinder at a temperature of -7°C, velocity of 64.3 m/s, LWC of 0.8 g/m^3, and MVD of 12 microns. It was found that for this particular case, the transition was well modeled using this method.

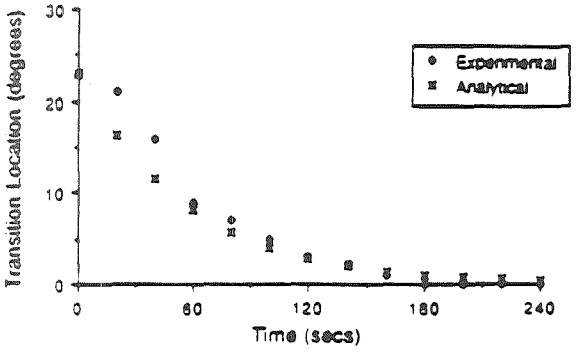

Fig. 2. Experimental and analytical surface roughness transition location on a 1" diameter cylinder with an assumed bead thickness of 2mm T = -7°C, V = 64.3 m/s, LWC = 0.8 g/m^3, MVD = 12 microns)

Because small time steps are used for some runs with LEWICE, a feature was added to the surface roughness transition model, where the surface runback water was allowed to "collect" at the interface for more than one time step, until there was enough surface water to form a bead. Once enough water has "collected" at the interface, the bead is added as frozen mass, and the boundary layer transition is set upstream of the bead.

3. Ice Shape Comparisons on Cylinders

In order to verify the effectiveness of the deterministic surface roughness transition model , ice accretion predictions for simple cylinders calculated by Multi-Zone LEWICE were compared to experimental ice shapes.

3.1. Initial Implementation of the Deterministic Model

An example of the initial implementation of the deterministic surface roughness transition model is shown in Fig. 3 for a 1" diameter cylinder at a temperature of -7°C, a velocity of 64.3 m/s, a LWC of 0.8 g/m^3, and a MVD of 12 microns. Based on observations of the surface roughness, the laminar roughness was set to k_l = 0.1mm, the turbulent roughness was set to k_t = 1mm, and the bead thickness was set to b = 2mm. In order to reduce the computational requirements during development of the transition model, the flow field was not recalculated for each time step. However, the ice accretion, heat transfer, and surface roughness components were updated at 20 second intervals. From Fig. 3 it can be seen that the Multi-Zone code with the deterministic surface roughness transition model is a significant improvement over the original Single-Zone LEWICE prediction which is shown in Fig. 3 for reference.

3.2. Effects of Flow Code Updates

Based on the positive initial results of the surface roughness transition model in the Multi-Zone code, a set of more complete runs were conducted with full updating of the flow field every time step. A number of difficulties were encountered in this process due primarily to numerical problems and limitations in the simple inviscid panel flow code used in LEWICE. One difficulty which occurred was a numerical instability resulting from the strong coupling between the flow velocity at the surface and the convective heat transfer. Due to the nature of the paneling method, the flow velocity at the surface exhibits high velocity spikes. Because the heat transfer increases with velocity, these spikes result in enhanced ice growth regions. In subsequent time steps, the flow is accelerated around these growths resulting in even further growth and instability. In the physical situation, regions of enhanced growth or roughness may occur but will not result in unstable growth due to lateral surface heat transfer (i.e. between adjacent elements) which is ignored in LEWICE. Lateral heat transfer would result in smoothing the heat transfer spikes. This was resolved in the model by including a smoothing routine in the local heat transfer calculation.

An example of the predicted ice accretion with flow updating and heat transfer smoothing is shown in Fig. 4 for the same conditions simulated in Fig. 3. It can be seen that some irregularity due to local heat transfer enhancement is still present and that the growth rate in the stagnation region is not as high as the experimentally observed case. The low stagnation growth rate is thought to be due to an underestimation of the flow velocity at the surface in the stagnation region after horn formation. Again, the inviscid panel code does not accurately reflect the flow in the concave stagnation region and the strong coupling between surface flow velocity and the local heat transfer coefficient results in a lower accretion rate. It should be noted that the local heat transfer coefficient is much more strongly dependent on the details of the flow near

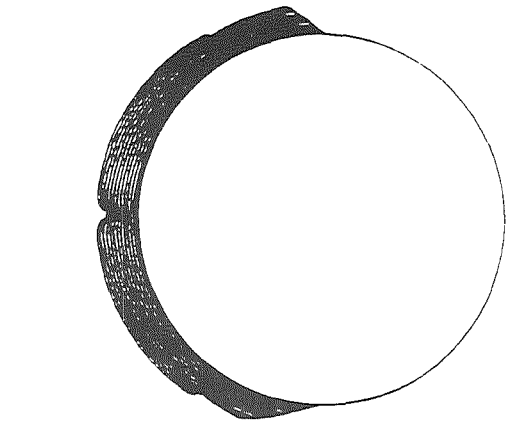

a. Original LEWICE prediction.

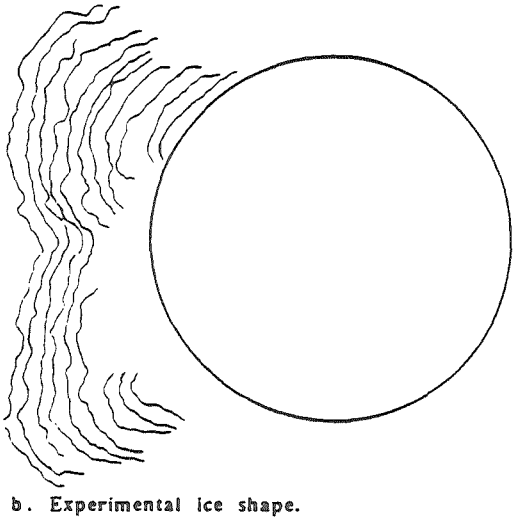

b. Experimental ice shape.

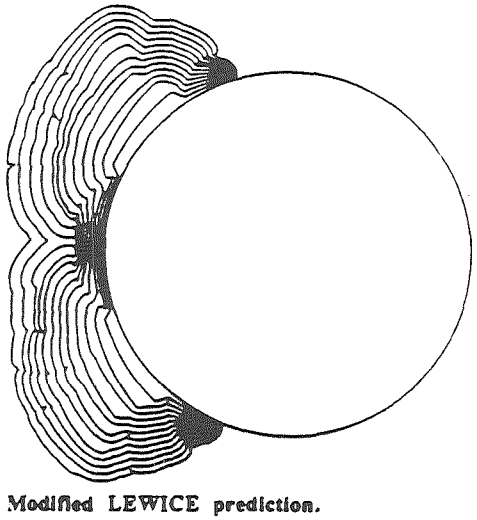

c. Modified LEWICE prediction.

Fig. 3. Comparison of experimental and predicted ice shapes for a 1" cylinder at 20 sec. intervals. (T = -7°C, V = 64.3 m/s, LWC = 0.8 g/m^3, MVD = 12microns, k_l = 0.1mm, k_t = 1mm, and b = 2mm)

the surface that the local droplet impingement efficiency for cloud size droplets.

Based on a comparison between Figs. 3 and 4, it appears that while both simulations do an adequate job, the single flow field case more closely replicates the experimentally observed ice accretion. However, care must be exercised in drawing conclusions from such comparisons between experimental and simulated ice accretions due to uncertainties in the experimental icing parameters and the limited number of cases available for comparison.

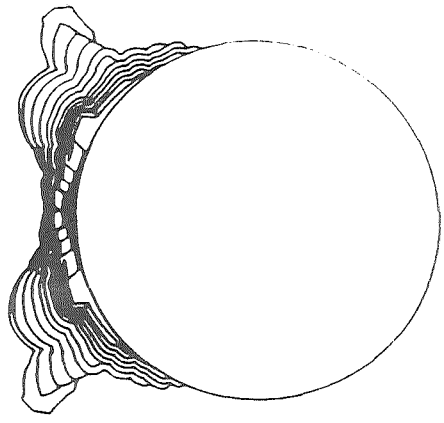

Fig. 4. Example of predicted ice accretion with flow updating for a 1" cylinder. (T = -7°C, V = 64.3 m/s, LWC = 0.8 g/m^3, MVD = 12 microns, k_l = 0.1mm, k_t = 1mm, and b = 2mm)

3.3. Effects of Other Factors

The effects of other input parameters on the predicted ice shapes were studied. It was found that increasing the thickness parameter b determines decreased the rate at which the transition location propagated toward the stagnation point. The turbulent roughness size k_t was found to only weakly influence the ice shape. This can be seen in Fig. 5, where the turbulent roughness size is increased from 1.35mm to 2.5mm for the conditions run in Section 3.1. Increasing the turbulent roughness size slightly increases the ice accretion in the rough region and limits the angular extent of the horns, but the overall ice shapes are remarkably similar. These factors are discussed more in detail in the next section, with examples of ice accretions on an airfoil.

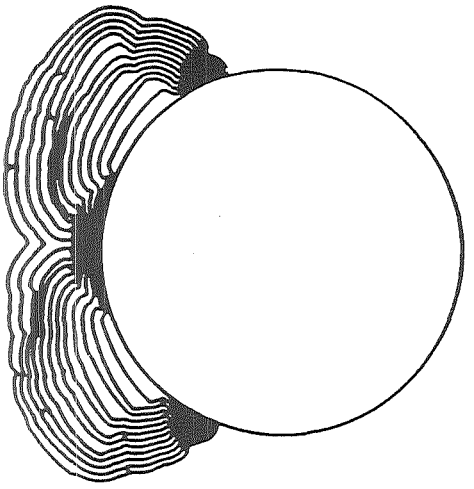

(a) k_t = 1.35mm

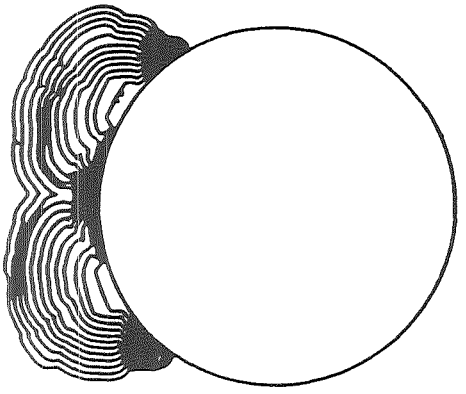

(b) k_t = 2.5mm

Fig. 5. Comparison of ice accretions for two values of turbulent roughness size (T = -7°C, V = 64.3 m/s, LWC = 0.8 g/m^3, MVD = 12 microns, k_l = 0.1mm, and b = 2mm)

4. Ice Shape Comparisons on Airfoils

The effectiveness of the deterministic Multi-Zone model for an airfoil geometry was tested on a NACA 0012. Runs were conducted to investigate the effect of the input parameters; namely, the laminar roughness size k_l, the turbulent roughness size k_t, and the bead thickness parameter b, on the predicted ice shapes. A series of 12 simulations were performed on a 30 cm chord NACA 0012 airfoil at 0° angle of attack. The icing conditions were the same in all of these runs: V = 29 m/s, LWC = 0.5 g/m^3, T_{amb} = 260.55°K, and MVD = 20 microns. These conditions correspond to the Example 1 from the LEWICE User's Manual[9] which is based on the 120 sec. experimental ice accretion measured by Gent et al.[10] and is shown in Fig. 6. The ice profiles and flow fields were calculated every 20 seconds and the simulations terminated at two minutes.

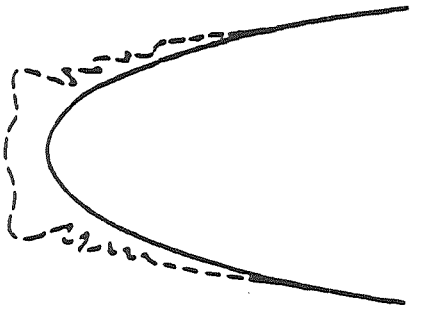

Fig. 6. Experimental ice accretion on a 30 cm chord NACA 0012 (α = 0°, T = -12.6°C, V = 129 m/s, LWC = 1 g/m^3, and MVD = 12 microns)

4.1. Effect of the Laminar Roughness Size

In order to investigate the effect of the laminar roughness size, k_l, was varied between 0.05mm to 0.35mm in the three runs, shown in Fig. 7. The other parameters were held fixed, with k_t = 0.35 and b = 1.0 mm. As shown in Fig. 1, the predicted ice shapes were strongly affected by the laminar roughness size. The simulation with the largest value of laminar roughness (Fig. 7a) produced the most "horn-shaped" ice structure (characteristic of glazed ice formations) while the runs with smaller value of laminar roughness (Figs. 7b, 7c) produced rougher, more "rime-type" ice accretions.

The difference in final ice profiles is attributed to changes in the *initial location* and the *subsequent motion* of the boundary layer transition point. It was found that the larger the laminar roughness size, the closer was the initial transition point to the stagnation region. For example, for a laminar roughness of 0.05 mm (Fig. 7c), the initial boundary layer transition point occurred at a distance seventeen segments (approximately 8.5 cm) downstream from the stagnation point and moved upstream to the ninth segment (approximately 4.5 cm) by T = 120 seconds. For the case with a laminar roughness of 0.10 mm (Fig. 6b), the boundary layer transition point started at segment 7 (approximately 3.5 cm) and moved to the stagnation region by t = 100 sec.). For Fig. 7a, having the largest value of the laminar roughness, virtually all of the airfoil surface was turbulent from the initial time step. It is believed that the increase in heat transfer in the turbulent region coupled with impingement effects causes greater ice growth and accounts for the horned structure.

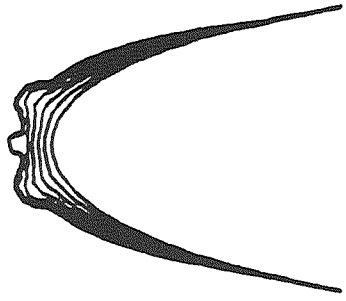

(a) k_t = 0.35mm

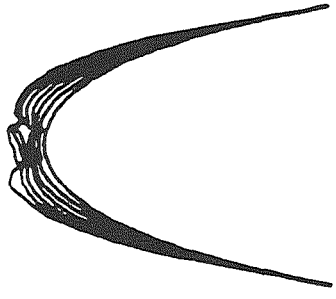

(b) k_t = 0.10mm

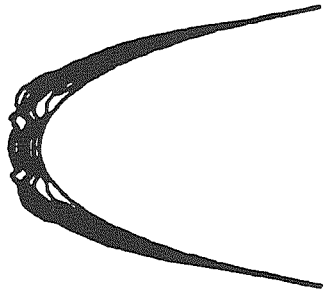

(c) k_t = 0.05mm

Fig. 7. Laminar roughness size influence on 120 sec. ice profiles

4.2. Effects of Turbulent Roughness Size

The effect of turbulent roughness size on ice shapes was investigated in the runs shown in Fig. 8. The laminar roughness and bead thickness parameter were the constant for all three cases, with values of 0.05 mm and 1.0mm, respectively, but the turbulent roughness was increased (k_t = 0.55mm) in Fig. 8b, and decreased (k_t = 0.15mm) in Fig. 8c, relative to the value used in Fig. 8a. Comparing the predicted ice profiles at t = 120 sec. shows that, as in the cylinder example in Section 3.3, the turbulent roughness size did not have much effect on the ice shapes. It is important to note that the initial transition location and the transition point motion were practically identical for all of these runs. The ice profiles are similar because all the water impinging on the surface in the turbulent region was

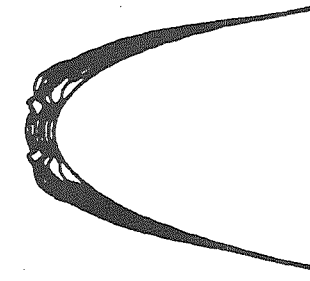

(a) k_t = 0.35mm

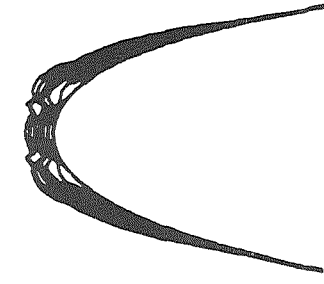

(b) k_t = 0.55mm

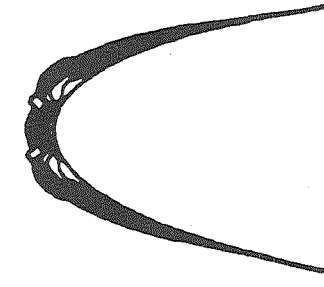

(c) k_t = 0.15mm

Fig. 8. Turbulent roughness size influence on 120 sec. ice profiles

frozen on impact. Therefore, although the larger roughness size increased the turbulent heat transfer, there was enough heat transfer, even with the smaller roughness sizes, to remove all of the latent heat of freezing. This is consistent with experimental observations at similar conditions where no surface water runback was found in the rough regions.[5] It also indicates that since all of the impinging water is frozen in the rough region, the amount of impinging water determines the amount of ice accreting in this region.

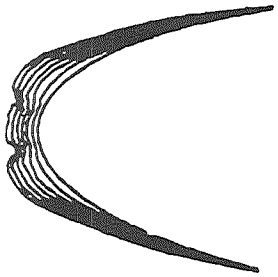

(a) k_t increases 0.1mm every 20 sec.

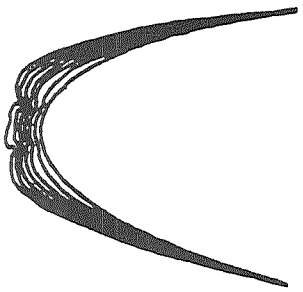

(b) k_t increases 0.2mm every 20 sec.

Fig. 9. Effect of increasing turbulent roughness size with time on 120 sec. ice profiles

Further evidence that indicates that the turbulent roughness has little impact on the resulting ice shape is shown in Fig. 9. These runs do not employ the deterministic model but, rather, are based on the simpler Multi-Zone model where the transition movement was controlled manually. The laminar roughness and the transition movement were identical in Figs. 9a and 9b, but the turbulent roughness differed. Initially, the turbulent roughness at the beginning of each simulation had the same value for both cases but changed with time at different rates. The turbulent roughness in Fig. 9a increased 0.1mm every 20 seconds but was ramped at twice this rate in Fig. 9b. Despite the differences in turbulent roughness, the resulting ice profiles are very similar.

4.3. Effects of the Bead Thickness Parameter

The final parameter investigated in this study was the bead thickness parameter b. The bead thickness is related to the size of the bead believed to be formed at the interface between the smooth and rough zones as discussed in Section 2.2. Its value determines the rate at which the transition location propagates toward the

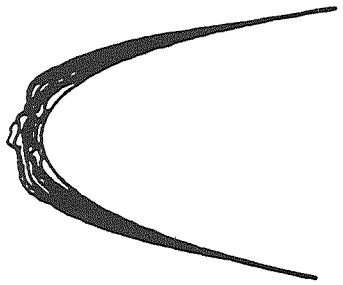

(a) Bead thickness parameter = 0.5mm

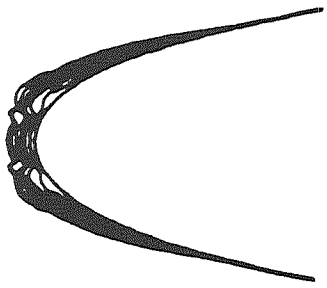

(b) Bead thickness parameter = 1.0mm

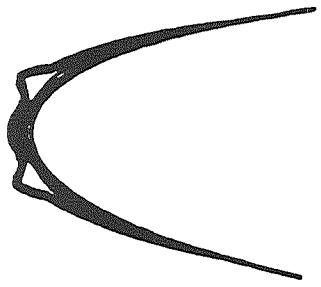

(c) Bead thickness parameter = 2.0mm

Fig. 10. Bead thickness parameter influence on ice profiles

stagnation point based on the amount of surface water flux. The effect of the thickness parameter on the ice shape was investigated in Figs. 10a, 10b, and 10c using the deterministic model with bead thickness values of 0.5mm, 1.0mm, and 2.0mm respectively. The laminar roughness and turbulent roughness were fixed and set to the same values used in Fig. 7c (k_l = 0.05mm, k_t = 0.35mm). Figure 10 compares the ice profiles at the same time and shows that the bead thickness parameter has major impact on the ice shape. (Note: because of a numerical instability, the Fig. 9c run was terminated at 100 seconds).

The profile changes drastically as the thickness parameter changes. A rime-type conformal ice accretion forms for the run with smallest value of bead thickness parameter (Fig. 10a), whereas horns clearly appear in the simulation with the largest bead thickness parameter (Fig. 10c). Since the initial transition location is the same in all of these runs (same laminar roughness), the difference in final ice shape profile is attributed to the *rate* at which the transition point propagates towards the stagnation point. The rate of propagation varies inversely with the bead thickness parameter. For thickness parameter = 0.5mm (Fig. 10a), the transition point moves upstream very quickly with time to the stagnation region. For thickness parameter 1.0mm (Fig. 10b), the transition point also moves continuously upstream with time but at a slower rate. For the largest value of thickness parameter, 2.0mm, the transition point has very little movement.

4.4 Experimental Comparison

In Fig. 11, the experimental ice shape is compared with the original Single-Zone LEWICE and the Multi-Zone LEWICE result from the case run in Fig. 9c. It can be seen that the Multi-Zone LEWICE reproduced the experimental ice shape somewhat better than the original LEWICE code. It should be noted that this case was used to calibrate the effects sand grain roughness k_s and was Example 1 in the original LEWICE manual. It is considered one of the best cases of agreement between the original Single-Zone LEWICE and an experimentally measured glaze ice accretion. Thus, it appears that the Multi-Zone model works well on airfoil geometries with a more complete physical model and more realistic values of the laminar and turbulent surface roughness. Further comparisons are needed, however, over a range of different icing conditions to establish the robustness of the method.

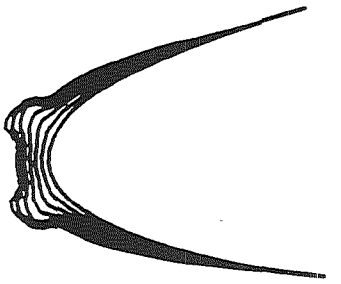

(a) Original Single-Zone LEWICE

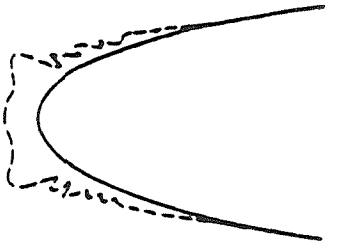

(b) Experimental Accretion

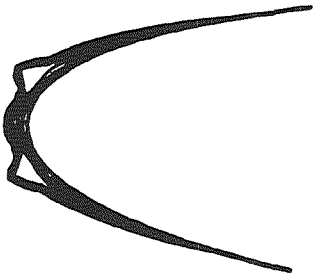

(c) Multi-Zone LEWICE

Fig. 11. Ice shape comparison for 30 cm chord NACA 0012

5. Conclusions

A deterministic surface roughness transition model was proposed and implemented in the Multi-Zone version of the LEWICE ice accretion prediction code for glaze ice conditions. The transition model links the smooth/rough surface roughness transition with the laminar to turbulent boundary layer transition. The initial transition location is determined by boundary layer stability in the smooth laminar region. The subsequent upstream migration of the transition region is caused by a surface water bead formation process and controlled by the surface water flux out of the laminar/smooth region. The effectiveness of the surface roughness transition model was tested by comparing predictions of the deterministic Multi-Zone LEWICE code with experimental ice accretions for cylinder and airfoil geometries. Good agreement was achieved between the deterministic Multi-Zone LEWICE predictions and the experimental ice shapes. Some numerical difficulties were encountered due to limitations of the flow field code used in LEWICE. The glaze ice shapes were found to be sensitive to the laminar surface roughness and bead thickness parameters which controlled the transition location. The ice shapes were found to be insensitive to the turbulent surface roughness.

Acknowledgements

This work was supported in part by the National Aeronautics and Space Administration and the Federal Aviation Administration under Grants NAG-3-666 and NGL-22-009-640. The work was also supported by the National Science Foundation Presidential Young Investigators Program, Award No. 8552702. Michael Kazmierczak was supported by the Ohio Aerospace Institute Investigators Program. The authors wish to thank Mark Potapczuk for his technical contributions.

References

1. Achenbach, E., "The Effect of Surface Roughness on the Heat Transfer from a Circular Cylinder to the Cross Flow of Air," International Journal of Heat and Mass Transfer, Vol. 20, 1977, pp. 359-369.

2. Yamaguchi, K. and Hansman, R.J., "Improved Ice Accretion Prediction Techniques Based on Experimental Observations of Surface Roughness Effects on Heat Transfer," MIT Aeronautical Systems Laboratory Report, ASL-90-5, 1990.

3. MacArthur, C.D., "Numerical Simulation of Airfoil Ice Accretion," AIAA Paper 83-0112, Jan. 1983.

4. Hansman, R.J., Yamaguchi, K., Berkowitz, B., and Potapczuk, M., "Modelling of Surface Roughness Effects on Glaze Ice Accretion," AIAA Paper 89-0734, Jan. 1989.

5. Olsen, W., and Walker, E., "Experimental Evidence for Modifying the Current Physical Model for Ice Accretion on Aircraft Surfaces," NASA TM-87184, 1986.

6. Yamaguchi, K. and Hansman, R.J., "Heat Transfer on Accreting Ice Surfaces," AIAA Paper 90-0200, Jan. 1990.

7. Messinger, B.L., "Equilibrium Temperature of an Unheated Icing Surface as a function of Airspeed," Journal of the Aeronautical Sciences, Jan. 1953, pp.24-42.

8. Hansman, R.J., and Turnock, S.R., "Investigation of Surface Water Behavior During Glaze Ice Accretion," AIAA Paper 88-0015, Jan. 1988.

9. Ruff, G.A. and Berkowitz, B.M., "Users Manual for the NASA Lewis Ice Accretion Prediction Code (LEWICE)," NASA C. R. 185129, 1990, p. 116.

10. Gent, R.W., Markiewicz, R.N., and Cansdale, R.T., "Further Studies of Helicopter Rotor Ice Accretion and Prediction," Paper 54, 11th European Rotorcraft Forum, Sept. 1988.